# Chapter 9
# Solar Cells

**Ching-Fuh Lin**

## Symbols

| | |
|---|---|
| kW | $10^3$ Watt |
| TW | $10^{12}$ Watt |
| kWh | Kilowatt hour |
| B | Boron |
| $\nu$ | Frequency of light |
| h$\nu$ | Photon energy |
| E | Energy |
| eV | Electron volt |
| nm | Nanometer |
| I | Electric current |
| $I_0$ | Dark current |
| $I_{pc}$ | Photo current |
| exp | Exponential |
| k | Boltzmann constant |
| T | Temperature |
| $V_{oc}$ | Open-circuit voltage |
| ln | Nature log |
| $I_{sc}$ | Short-circuit current |
| R | Resistor |
| I-V | Current-voltage |
| V | Voltage |
| $P_m$ | Maximum power |

C.-F. Lin (✉)
Innovative Photonics Advanced Research Center, Graduate Institute of Photonics and Optoelectronics, Department of Electrical Engineering, National Taiwan University, Taiwan, No. 1, Sec. 4, Roosevelt Rd, Taipei 10617, Taiwan
e-mail: lincf@ntu.edu.tw



C.-C. Lee (ed.), *The Current Trends of Optics and Photonics*,
Topics in Applied Physics 129, DOI 10.1007/978-94-017-9392-6_9

| | |
|---|---|
| $I_m$ | Maximum current |
| $V_m$ | Maximum voltage |
| FF | Fill Factor |
| $\eta$ | Efficiency |
| $P_{in}$ | Power input |
| Ec | Conduction band |
| S | Ground state |
| $S^*$ | Excited state |
| h | Planck constant |
| μm | Micrometer |
| $I^-$ | Iodide ion |
| $I_3^-$ | Triiodide ion |
| $e^-$ | Electron |
| Pb | Lead |

## 9.1 Introduction

Since 1765, the world had been reshaped with the steam engine invented by James Watt. This is generally known as the first industrial revolution. After then, human labors and animal power were replaced with machines and fossil energy became the major resources to power modern industry. Energy consumption from fossil fuels that include coal, oil, and natural gases grows almost 40 times from 1900 to 2000. No reverse trend is foreseen in the near future.

The use of fossil energy for more than one hundred years had created three crises. The first is certainly the possible depletion of fossil energy. The second is the global warming due to the emission of greenhouse gases. The emission of carbon dioxide reached the historical record of 30,600 million tons in 2010. In comparison, it was less than 15,000 million tons in 1970. Even the worse, after 2004, non-OECD countries generated more carbon dioxide than OECD countries. Such fact certainly worsens the emission of carbon dioxide. Many experts attribute the global worming to the emission of greenhouse gases like carbon dioxide. A recent report from NASA, USA, states that the global temperature has an obvious increase since 1980. As compared to the average temperature between 1951 and 1980, the global temperature has increased 0.5–0.6 °C. The north hemisphere has even more increase. Many glaciers disappeared. The worst part is that, on Greenland, the ice melts to dilute and lower the salinity of the Arctic sea and then significantly influences the conveyed ocean currents.

The global warming had further led to the third crisis of dramatic weather change. Many places have record rainfalls or extreme wind speed in recent years. For example, the Mississippi River in the United States had huge floods in April

and May 2011 because two major storms created record levels of rainfall. Such flood spread over several states, including Missouri, Illinois, Kentucky, Tennessee, Arkansas, Mississippi, and Louisiana. In the coming year, October, 2012, hurricane Sandy also severely damaged east coast of the United States. Its wind diameter is nearly 2,000 km, covering a broad range of area, from eastern part of the US and Canada. It affected twenty-four states, including south state of Florida and the north state of Maine. Although it is controversial to directly attribute the dramatic weather change to global warming, such phenomena cannot be experimented in the laboratory. The coincidence between the temperature rise and the detrimental weathers in recent years give us a strong warning. It is time for us to reduce global warming. Therefore, using other energy resources that do not emit greenhouse gases to replace fossil energy is an important issue.

Solar, hydropower, ocean wave, tide, biomass, wind, and geothermal energies are all included in renewable energies. Hydropower has a long history of being used by human beings and still generates about 15 % of global electricity. Unfortunately, hydropower relies deeply on large rivers with steady water current. Ocean waves and tides need to take into account the corrosion of salty water and are still not mature enough for practical implementation. Biomass needs huge lands to grow plants and could possibly cause food crisis due to its land competition with agricultural crops. Geothermal also relies on particular areas that are closely linked to earthquake zones. Thus, among all renewable energies, wind and solar are probably the two mostly developed technologies that have the potential to generate significant electricity worldwide. The global wind power has the potential of approximately $1.3 \times 10^{16}$ kW. This amount is about 850 times of global power demand nowadays. Some estimate that about 72–170 TW is extractable in a cost-competitive manner. This amount is still much larger than human needs. However, the wind power is usually not stable and dramatically influenced by geographical conditions.

In comparison with other renewable energies, solar energy has more advantages. First, it is almost everywhere. For the most populated areas, from equator to 40° of latitude, sunshine is abundant. Second, solar power is 174,000 TW. The human demand of power is about 16 TW, so solar energy is about 11,500 times of human needs. With the solar intensity of 1 kW/cm$^2$ and 15 % of efficiency, to generate 16 TW of power for global consumption, we need an area of about $1 \times 10^5$ km$^2$, which is only 0.07 % of total land area on earth surface. For a regular house with 100 m$^2$ roof, even with only 10 % efficiency, using solar panels on the roof will give 10 kW of power. If the house is in the region that has 3.5 h of equivalent sunshine, it will have 35 kWh of electricity each day. Then it will generate energy of over 1,000 kWh per month. Such energy can sufficiently provide the need for a usual household.

Because solar energy has the above potential, this chapter will focus on the topic of solar cells. We will start with the operation principles. Then several types of solar cells will be discussed in depth.

## 9.2 Principles of Solar Cells

### *9.2.1 Semiconductor p-n Junction Solar Cells*

The first solar cell had been invented for more than 70 years. In 1940, R. Ohl discovered that the silicon p-n junction was light sensitive [1]. He patented it in 1941. Then D. Chapin, C. S. Fuller and G. Pearson reported 4.5 and 6 % from a silicon solar cell [2] in 1954. This solar cell was also based on p-n junction. The first energy crisis in 1973 had sparked the fast development of solar cells, so less than 15 years later the first Si solar cell beyond 20 % was reported in 1985. The Si-based solar cells are still the main stream of commercial use. Other semiconductor types of solar cells are also rapidly developed. They all have similar operation principles that are based on p-n junction. Therefore, the operation principle of semiconductor p-n junction solar cells will be first discussed here.

Before discussing p-n junction, we shall review p-type and n-type semiconductors briefly and take Si as an example of semiconductors to understand their characteristics. A silicon semiconductor that is not doped with any impurity is called intrinsic. When an intrinsic Si semiconductor is doped with impurity atoms that have one more electron than Si in the outer electronic orbit, e.g. P, then there will be more electrons than holes. This extra electron can move freely in the semiconductor. Because electron is negatively charged, such doped semiconductor is called n-type semiconductor. However, the n-type semiconductor is not negatively charged. The atom with one more electron than Si becomes positively charged when this extra electron leaves it. The extra electrons and the positively charged atoms are equal in numbers, so the overall charge of the semiconductor is neutral.

Similarly, when an intrinsic Si semiconductor is doped with impurity atoms that have one electron less than Si in the outer electronic orbit, e.g. B (Boron), there will be less electrons than holes. A hole represents that the orbit is lack of an electron. Thus a hole is positively charged and such semiconductor is thus called p-type. The electron in the neighboring locations can move to this orbit that is lack of an electron. This is equivalent to hole moving to another location. Therefore a p-type semiconductor has more holes than electrons. Also, the p-type semiconductor is not positively charged. Because the atom with one electron less than Si becomes negatively charged when another electron comes to fill up this orbit. The numbers of the holes and the negatively charged atoms are equal, so the overall charge of the semiconductor is neutral.

A p-n junction is formed when a p-type semiconductor and an n-type semiconductor are brought together to have a close contact. Figure 9.1 shows a schematic of the p-n junction. Near the junction, the holes in the p-type semiconductor diffuse to the n-type semiconductor because the hole concentration there is higher than the n-type semiconductor. As holes move to the n-type semiconductor, the left-behind atoms become negatively charged ions. Similarly, electrons in the n-type semiconductor diffuse to the p-type semiconductor, so the atoms there become positively charged. Although the positively charged ions and the

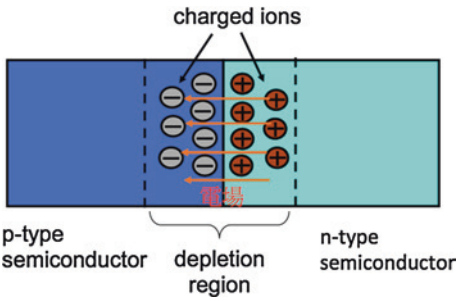


**Fig. 9.1** A schematic of the semiconductor p-n junction

negatively charged ions are close near the p-n junction, they cannot move because those ions are located at the lattice sites in the semiconductor crystal. However, the positively charged ions and the negatively charged ions will create a huge electric field, called built-in field. The region that is occupied with the charged ions is called depletion because there are very few electrons and holes in this region. Thus the built-in field is in the depletion region. The direction of the field is indicated by the arrow signs in Fig. 9.1.

This built-in electric field in the depletion region is very important for the operation of semiconductor p-n junction solar cells. First, let's assume that an extra electron-hole pair is generated in the depletion region no matter how it is generated. Because this field is very strong, the electron and the hole will be pulled away and transport toward opposite directions. Electron will be forced to move to the n-type semiconductor and the hole is pulled toward the p-type semiconductor.

Next, let's discuss how the extra electron-hole pair is generated. One of the possibilities is that the p-n junction is illuminated by light. In this case, light is usually viewed as a collection of many photons. The energy of a photon is proportional to the light frequency. If the frequency of light is $\nu$, then the corresponding photon energy is equal to $h\nu$, i.e., $E = h\nu$. If the energy of photon is larger than the bandgap of semiconductors, it can be absorbed and cause the electron in the valence band to transit to the conduction band. That is, an electron in the conduction band and a hole in the valence band are generated. From this point of view, the bandgap of semiconductor is an important factor that influences the absorption of light in the semiconductors. For Si, its bandgap is 1.12 eV, so light with energy $E = h\nu > 1.12$ eV will be absorbed. In other words, if the wavelength of light is less than 1,100 nm, it can be absorbed by Si.

The photo-generated electron-hole pair can form an exciton, which is a particle similar to a hydrogen atom with the negatively charged electron orbiting around the positively charged hole. The exciton has an energy less than an electron-hole pair that is not bonded. This energy is called binding energy of exciton. In semiconductors, the exciton binding energy is small. For example, in Si, it is only 15 meV. This energy is much smaller than thermal energy, so most of the excitons in Si will dissociate and become freely moving electrons and holes. Then those electrons and holes will move according to what is described previously.

On the other hand, if extra electron-hole pairs are generated outside of the depletion region, what will happen? Let us take n-type semiconductor as an example. When there are more electrons in the n-type semiconductors at a certain location, those electrons will diffuse. Similarly, when there are more holes than background, those holes will diffuse. Nonetheless, because holes are minority carriers in the n-type semiconductor, they will recombine with electrons sooner or later, depending the diffusion length or carrier lifetime of holes therein. If those holes are able to diffuse to the depletion region, they will not be recombined. Instead, the built-in electric field will pulled them toward the p-type semiconductor. If the distance between the depletion region and the location that extra holes are generated is less than the diffusion length, the extra holes will very likely move to the depletion region before being recombined with electrons. As a result, the carrier lifetime or diffusion of minority carriers is a very important parameter for semiconductors. Similarly, as extra electron-hole pairs are generated in the p-type semiconductors, extra electrons will be recombined if they cannot diffuse to the depletion due to recombination with holes. On the contrary, if the location that generates extra electrons is within the diffusion length from the depletion region, the electrons are most likely able to move to the depletion region and then pulled by the electric field toward the n-type semiconductor. From another point of view, if the minority carriers, i.e., electrons in the p-type semiconductor or holes in the n-type semiconductor, are generated at the locations that are far from the depletion region, more than the diffusion distance, they will mostly recombine with majority carriers and disappear, so cannot move to the opposite side of the p-n junction.

As mentioned previously, if extra electrons or holes are generated in the depletion region or at a location not far from the depletion region, they will possibly move to the opposite side of the p-n junction and then accumulate there. Now if the p-n junction is connected through an external circuit, as shown in Fig. 9.2, the accumulated electrons in the n-type semiconductor can flow through the circuit to the p-type semiconductors and then recombine with holes there. The accumulated holes in the p-type semiconductor recombine with electrons and disappear. This process gives us the current in the external circuit, which can be utilized for practical applications. This current is generated from the light illumination and so called photo current, usually indicated as Ipc.

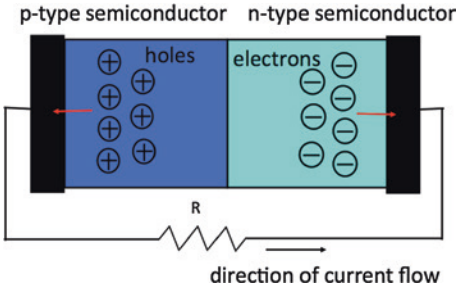


**Fig. 9.2** A p-n junction is connected through an external circuit

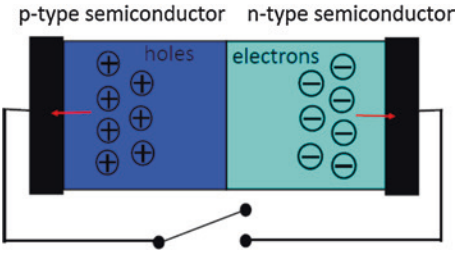


**Fig. 9.3** A p-n junction under open circuit

However, if the p-n junction is not connected externally, it becomes open circuit, as shown in Fig. 9.3. Then there will be no current flowing through the external circuit. As a result, electrons and holes that transport to the n-type and p-type semiconductors, respectively, will accumulate there. Because electrons and holes are charged particles, they will give rise to another field and a measurable voltage from the external circuit. This field can counter-balance the built-in field in the depletion region. Thus, when the forces from these two fields are equal, electrons and holes will not move further to cross the p-n junction. The voltage between the p-type semiconductor and the n-type semiconductor is given implicitly in the following formula.

$$I = I_0[\exp(\frac{eV}{kT}) - 1] - I_{pc} = 0 \tag{9.1}$$

where $I_0$ is the dark current.

In (9.1), the current consists of two parts. One is the photo current. The other is the current due to the voltage between the p-type semiconductor and the n-type semiconductor. As explained previously, when light is illuminated on the semiconductor, electrons will move toward the n-type semiconductor and vice versa for holes. Hence the photo current flows from the n-type semiconductor to the p-type semiconductor. However, for the current due to the voltage between the two types of semiconductors, because positively charged holes accumulate in the p-type semiconductor, the voltage is higher at this side than the other side of n-type semiconductor. The induced current has the direction from the p-type semiconductor to the n-type semiconductor. Therefore, the two currents have the opposite directions and the total is then given by (9.1). When the external circuit is open, because there is no current passing through the external, the total current is equal to zero. This leads to the open-circuit voltage given as follows.

$$V_{oc} = \frac{kT}{e} \ln\left(\frac{I_{pc}}{I_0} + 1\right) \tag{9.2}$$

On the other hand, if the resistor in Fig. 9.2 has zero resistance, it becomes short-circuit. Then the voltage across the p-type semiconductor and the n-type semiconductor is zero. The current is represented as Isc. According to (9.1), this current is given by

$$I = I_{sc} = I_{pc} \tag{9.3}$$

The direction of current flow in the external circuit is from the p-type semiconductor to the n-type semiconductor. Substituting (9.3) to (9.2) gives the following equation.

$$V_{oc} = \frac{kT}{e} \ln\left(\frac{I_{sc}}{I_0} + 1\right) \tag{9.4}$$

Thus the short-circuit current, Isc, and the open-circuit voltage, Voc, are not independent. In typical applications, the solar cell is connected to some appliance in the external circuit. This appliance can be represented by a resistor, R, as shown in Fig. (9.2). Then the relation between the voltage and the current is given by

$$I = I_0[\exp(\frac{eV}{kT}) - 1] - I_{sc} \tag{9.5}$$

In (9.5), the direction of current is defined as from the p-type semiconductor to the n-type semiconductor inside the p-n junction, so its direction is opposite to the arrow sign shown in Fig. 9.2. The current-voltage (I-V) curve is schematically shown in Fig. 9.4. This curve has an interception with the horizontal axis at Voc and an interception with the vertical axis at Isc. The actual operation point depends on the resistor in the external circuit. The relation of voltage and the current of the resistor is given by

$$\mathrm{V} = \mathrm{IR} \tag{9.6}$$

Here the direction of current I is the same as the arrow sign shown in Fig. 9.2. To make the two equations (9.5) and (9.6) have the same direction of current flow, (9.6) should be replaced with (9.7).

$$\mathrm{V} = -\mathrm{IR} \tag{9.7}$$

The operation point is the interception of the two curves from (9.5) and (9.7), as shown in Fig. 9.5. This point will certainly vary with the resistance. At one extreme, if the resistance is zero, the curve of V = IR is the vertical axis. Then the interception is at I = Isc and V = 0. Because V = 0, there will be no output power. For another extreme, if the resistance is infinite, then I = 0, so the curve of V = IR is the horizontal axis. The interception becomes I = 0 and V = Voc. There will be no output power, either, because there is no output current.

The above two cases are extreme situations. In practical conditions, the curve of V = −IR, which is actually a straight line, locates between the vertical axis and

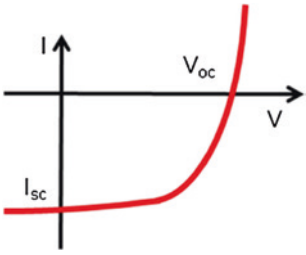


**Fig. 9.4** Current-voltage curve of a solar cell under light illumination

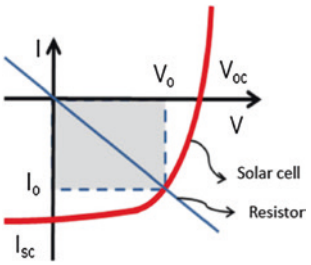


**Fig. 9.5** Current-voltage curve of a solar cell intercepts with the curve of an external resistor

the horizontal axis. As schematically shown in Fig. 9.5, the output voltage is Vo and the output current is Io. The output power is given by $P_o = I_o V_o$. As we vary the resistance R, the output power will vary and has a maximum, denoted as $P_m$. Its corresponding voltage and current are $V_m$ and $I_m$, respectively.

$$P_m = I_m \times V_m \tag{9.8}$$

The maximum power is less than the product of Isc and Voc. The ratio of Pm to the product of Isc and Voc is named as Fill Factor (FF).

$$FF = \frac{P_m}{I_{sc} V_{oc}} = \frac{I_m V_m}{I_{sc} V_{oc}} \tag{9.9}$$

Therefore, the output power Pm can be written as Pm = Isc × Voc × FF.

The efficiency of a solar cell, η, is then given by

$$\eta = \frac{P_m}{P_{in}} = \frac{I_m V_m}{P_{in}} \tag{9.10}$$

where $P_{in}$ is the incident power of sunshine. Because solar intensity varies with the latitude and weather, it is not a constant value. To make the evaluation of solar cells trustful, a standard solar intensity is defined as 100 mW/cm$^2$ or 1 kW/m$^2$. Hence, the evaluation of solar cells is usually taken from a unit area.

### *9.2.2 Organic Solar Cells*

Organic solar cells had been developed before 1983 [3]. The first noticeable device of organic solar cells was the two-layer structure with 1 % efficiency discovered by Tang [4] and then 5 % device invented in 2000 [5]. By convention, organic solar cells are made of organic materials that are conductive. Organic materials differ from usual inorganic semiconductors in several aspects. First, conductive organic materials have much smaller mobility than inorganic semiconductors. Second, the binding energy of excitons in organic materials is much larger than that in inorganic semiconductors. Third, the lifetime and the diffusion length of excitons in organic materials are much shorter than the lifetime and the diffusion length of carriers in inorganic semiconductors. Such differences make

the operation principle of organic solar cells different from semiconductor p-n junction solar cells. However, there is one similarity between these two types of materials. They have a bandgap. For inorganic semiconductors, the bandgap is the energy difference between the edge of the conduction band and the edge of the valence band. For organic materials, the bandgap is between the lowest unoccupied molecular orbital (LUMO) and the highest occupied molecular orbital (HOMO). Similar to the edge of the conduction band, LUMO is the lowest energy level of a group of closely spaced energy levels. Also, HOMO is the highest energy level of a group of closely spaced energy levels. Between LUMO and HOMO, there are no energy levels.

There are also two types of organic materials, named donor and acceptor. Donor is the kind of molecules that are easier to give away electrons than accepting electrons when they are close to another type of molecules. On the contrary, acceptor is the kind of molecules that easily receive electrons. Whether a molecule is easy to give away or to receive electrons is determined by the electronegativity. The larger the electronegativity of a molecule is, the more it is likely to attract electrons. Thus a donor has a smaller electronegativity than an acceptor.

Because the binding energy of excitons in organic materials is large, it is unlikely that electrons and holes are unbounded. Hence there are not many freely moving electrons and holes in organic materials. Therefore, when the donor and the acceptor are in touch with one another, electrons and holes do not move from one side to anther like in semiconductors. Therefore, there is no depletion region. As a result, there is no built-in field to pull electrons from the donor to the acceptor and to pull holes from the acceptor to the donor. Then how excitons dissociate and release electrons and holes? Also, how electrons and holes are separated and move toward the opposite directions to form current flow in the external circuit?

First, the organic solar cells have two electrodes of anode and cathode with different work functions. Usually anode has a higher work function than the cathode. In equilibrium, the work function will be forced to be at the same energy, so causing the energy levels to tilt, as shown in Fig. 9.6a. The tilted energy levels make electrons tend to move toward the cathode and the holes toward anode. The tiled energy field also indicates that there is an electric field between the anode and the cathode. However, this field is not as strong as the built-in field in the depletion region of the p-n junction in semiconductors. Next, when a photon incident on the donor, it will be absorbed and cause the electron below the HOMO level transit to the energy level above the LUMO level, as shown in Fig. 9.6b, leaving the empty energy level near the HOMO level, which is equivalent to a hole. Then in a very short period of time, the electron and hole will form an exciton. The electron in the exciton corresponds to an energy level lower than the LUMO level, as shown in Fig. 9.6c. An exciton has neutral charge, so it is actually not influenced by the tilted energy level. The excitons may move toward all directions. Here we focus on those that move toward the interface between the donor and the acceptor, as shown in Fig. 9.6d. If the energy level of the electron in the exciton is larger than the LUMO level of the acceptor, this electron will transit to the LUMO level of acceptor, as shown in Fig. 9.6e. At this point, the electron and the hole will separate. That is

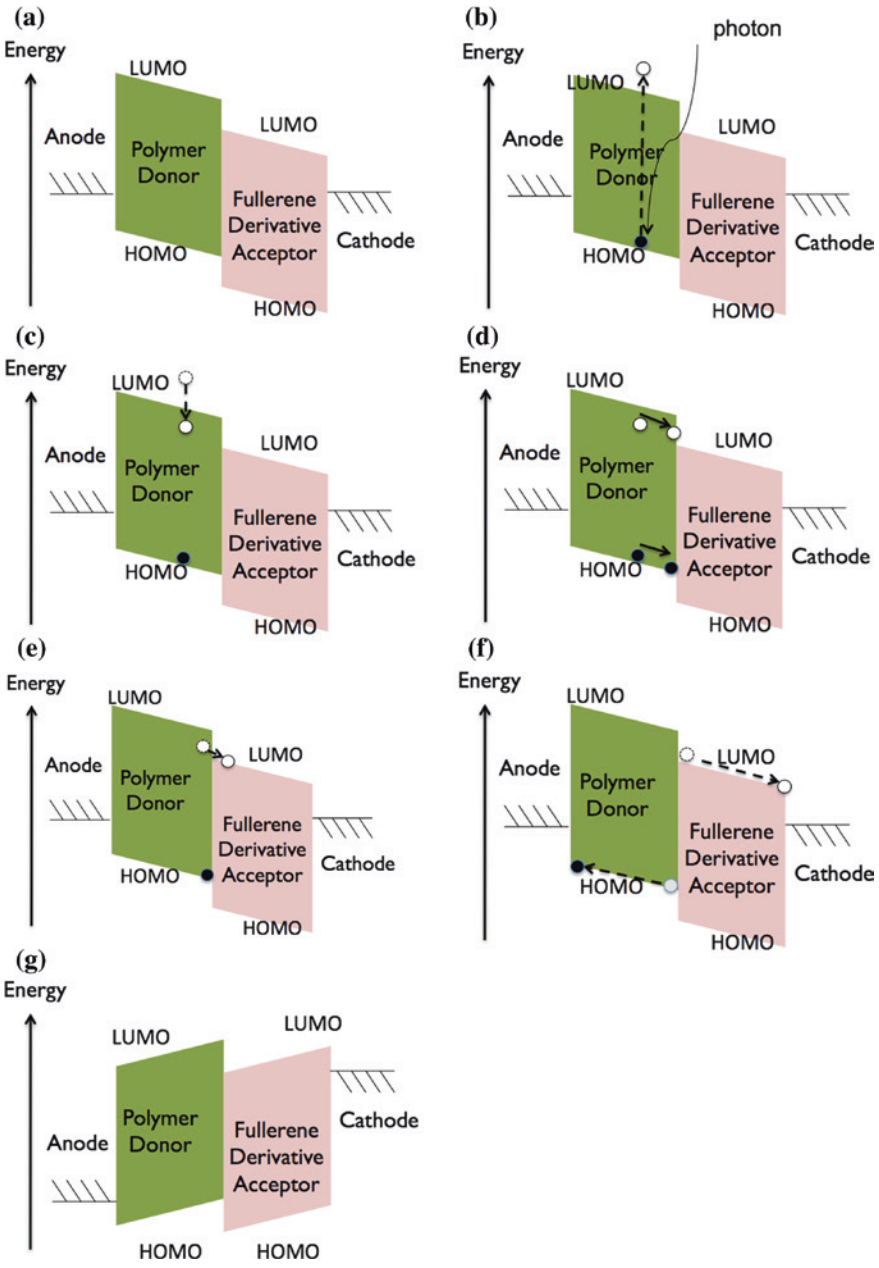


**Fig. 9.6** **a** Schematic energy levels of an organic solar cell; **b** incidence of a photon causing the electron under the HOMO level to transit to the high energy level; **c** the electron at the high energy level relax to another energy level lower than the LUMO level of donor-; **d** the electron and the hole forms an exciton and move toward the interface of the donor and the acceptor; **e** at the interface, the electron transit to the LUMO level of the acceptor; **f** the separated electron and hole transport toward the opposite directions; **g**) under open circuit, electrons and holes accumulate in the acceptor and the donor-, respectively, causing the energy levels to reverse the tilting direction

the exciton dissociate at the interface of the donor and the acceptor. As long as the electron and the hole are separated, they will move to the opposite electrodes, as shown in Fig. 9.6f, due to two reasons. One is the tilted energy level or the electric field that pulls the electron to the cathode and the hole to the anode. The other is caused by the diffusion because there are more electrons near the interface of the donor and the cathode than near the electrode and similarly for holes.

If the organic solar cell is connected with an external circuit, the electrons near the cathode will pass through this external route to the anode and recombine with holes in the donor. If the organic solar cell is under open circuit, electrons and accumulate in the acceptor and holes will accumulate in the donor. Because of the negative charge of electrons and the positive charge of holes, they will build an electric field that has the direction opposite to the one set up by the cathode and anode. In the extreme case, it will be even larger than the original one, making the energy levels tilted oppositely, as shown in Fig. 9.6g. Such tilted energy levels will stop electrons further move to the acceptor and prevent holes from moving toward the anode, so there will be zero current at the open-circuit voltage. Its I-V curve will be similar to the one shown in Fig. 9.4 for the semiconductor p-n junction.

As mentioned previously, the photo-generated excitons can move toward all directions. If they move toward the anode instead of the donor-acceptor interface, the electron in the exciton will relax to the lower energy levels in anode, too, leading the dissociation of exciton, while holes will also move to anode. Then electrons and holes will recombine quickly in the anode, so there will be no current generated. To avoid this situation, a sandwiched structure is proposed. In this structure, two more layers are added to sandwich the donor and the acceptor materials. The energy diagram is shown in Fig. 9.7. The additional layer placed between the anode and the donor is called the electron-blocking layer. It has a conduction-band edge higher than the LUMO of donor, so electrons are blocked. Also, the exciton cannot dissociate and is bounced back, then moving toward the donor-acceptor interface. Similarly, the layer inserted between the cathode and the acceptor has a valance-band edge much lower than the HOMO of the acceptor, so holes are blocked. It is hence called hole-blocking layer. This layer is particularly important if the acceptor also absorbs light and exciton can be generated in this layer. The process is similar to the one described for the donor.

The above description is still too ideal. Because the exciton of organic materials has very short diffusion length, typically around 10 nm or less, most of the excitons will disappear before they move to the donor-acceptor interface if the thickness of the donor is larger than 20 nm. As a result, only those excitons generated approximately within 10 nm from the donor-acceptor interface can dissociate and contribute to the photo current. Those that are generated far from the interface will disappear. If the layer of donor is thick and light is incident from the donor side, most of light will be absorbed by the donor material near the anode. Although they will generate excitons, but very few are able to move to the interface without recombination. To increase the ratio of excitons able to reach the donor-acceptor interface, the layer of the donor has to be thin. However, a thin donor- layer cannot absorb much light, so not much light is converted to electricity. This becomes a contradictory condition.

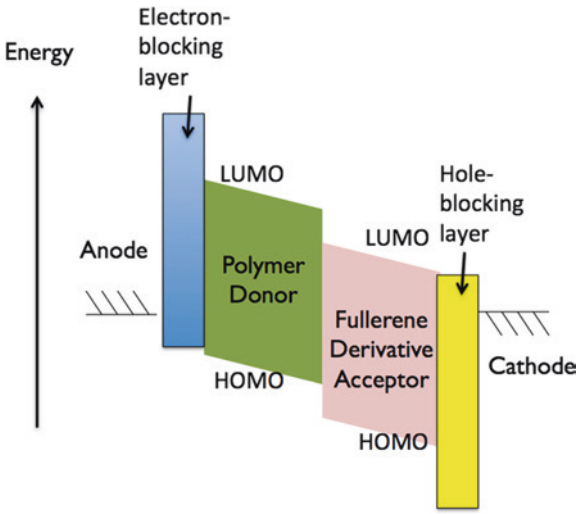


**Fig. 9.7** Band diagram with two more layers added to sandwich the donor- and the acceptor materials

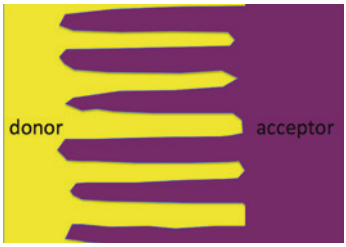


**Fig. 9.8** Inter-penetrated nano-network of the donor- and the acceptor

To overcome this deadlock, a bulk heterojucntion structure is proposed. A schematic of the structure is shown in Fig. 9.8. In this structure, the donor and the acceptor inter-penetrate into each other with many fingers. Ideally, each finger has the cross section of less than 20 nm, so the photo-generated excitons can meet the donor–acceptor interface quickly to provide fast dissociation of excitons. In the meantime, the effective thickness of the donor- and the acceptor is increased, so the light absorption is also increased. The structure in Fig. 9.8 is usually called inter-penetrated nano-network because those penetrated fingers are in the nanometer scale.

### *9.2.3 Hybrid Heterojunction Solar Cells*

Hybrid heterojunction solar cells include several types. Here we focus on the type that consists of an inorganic semiconductor and an organic material. The heterojunction formed by an inorganic semiconductor and an organic material is different from the semiconductor p-n junction. Figure 9.9a schematically shows the relative energy levels of the two materials before they are in contact. Here we use

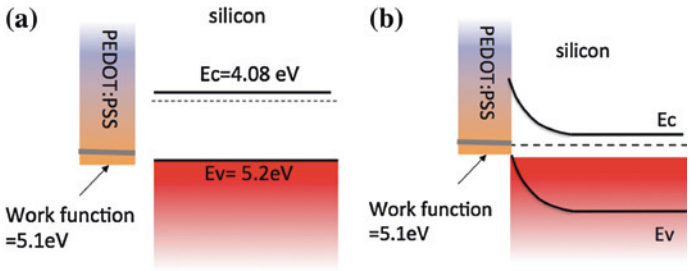


**Fig. 9.9** **a** The relative energy levels of Si and PEDOT:PSS; **b** The band diagram when the system is in equilibrium

the example with the junction formed from the n-type silicon and poly(3,4- ethyle nedioxythiophene):poly(styrenesulfonate) (PEDOT:PSS). When the two materials are brought to contact one another, they will interact and then achieve equilibrium. Because the work function of PEDOT:PSS is very close to the valence-band edge of Si, the excitons in PEDOT: PSS can possibly dissociate and the corresponding holes may transport to Si. As the holes move to n-type Si, they will quickly recombine with an electron. As a result, the bands of Si near the interface will bend, as shown in Fig. 9.9b. Because the electrons near the interface are recombined with holes, there will be much less electrons. There will be also a depletion region due to the lack of electrons. There will also be a built-in field in the depletion region, which mainly locates in the silicon side.

As light is illuminated on the Si, it will be absorbed and electron-hole pairs will be generated. Because of the band bending, electrons will be forced toward the electrode at the Si side and holes will move to PEDOT:PSS and then to the electrode connected with PEDOT:PSS. If the solar cell is connected with an external circuit, electrons will pass through it, then enter the PEDOT:PSS, and recombine with holes there. If the solar cell is under open circuit, electrons will accumulate in Si, while holes will accumulate in PEDOT:PSS. The accumulate electrons and holes at the opposite sides will create another field to balance the original built-in field, leading to the flat band and so a measurable open-circuit voltage.

### *9.2.4 Dye-Sensitized Solar Cells*

The conventional device structure of a dye-sensitized solar cell (DSSC) consists of the mesoporous TiO film, the dye adsorbed on the $TiO_2$ film, the iodine based redox electrolyte ($I^-I_3^-$ electrolyte), and the counter electrode, as shown in Fig. 9.10.

The mesoporous TiO film is usually coated on a fluorine-doped SnO transparent electrode (FTO) as the photoelectrode. The process starts from coating $TiO_2$ paste. The paste is then sintered at 450–500 °C. It produces a $TiO_2$ film with thickness of ~10 μm. Then the dye is adsorbed on the surface of the porous structure of the $TiO_2$ film. Because this mesoporous film is composed of $TiO_2$ nanoparticles

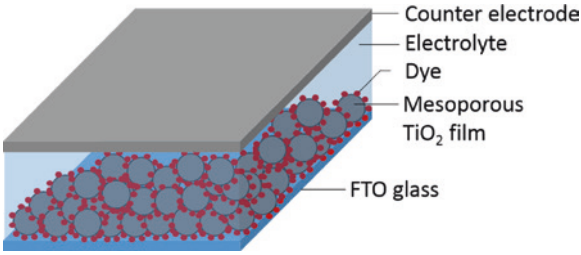


**Fig. 9.10** The conventional device structure of DSSC

(~10–30 nm), it has huge surface area and the amount of dye adsorbed is very large. The amount of dye adsorbed significantly influences the light harvesting efficiency. Practically, in order to scatter the incident light effectively to increase the light absorption, this $TiO_2$ film normally contains large $TiO_2$ particles (~250–300 nm). Theoretically, the larger thickness of $TiO_2$ film is expected to adsorb more dyes. However, a thick film may increase the charge recombination between the injected electrons and the dye due to the numerous grain boundaries between $TiO_2$ nanoparticles and the low electron diffusion coefficient in the $TiO_2$ film [6]. Thus the $TiO_2$ film should be controlled to near the optimized thickness [7].

For the adsorption of dye, the dye is attached to the $TiO_2$ surface through the carboxyl groups ($COO^-$ and COOH moieties). It can be verified by Raman spectroscopy [8]. Under the illumination of light, in the anode, the excited electron is injected from the dye to the $TiO_2$ photoelectrode. For the typical Ru complex dye, the metal-to-ligand charge-transfer (MLCT) transition is observed [9]. Furthermore, in the cathode, the transition of electrons between the dye and the counter electrode is conducted by the electrolyte. Typical electrolyte used in the DSSC contains $I^-/I_3^-$ redox ions. Pt-coated TCO substrate is usually used as the counter electrode.

The operation principle of the DSSC and the energy band diagram are illustrated in Fig. 9.11.

Under the illumination, the dye is excited from the ground state (S) to the excited state ($S^*$).

$$S + h\nu \rightarrow S^*$$

The excited electrons are injected into the conduction band of the $TiO_2$ photoelectrode, resulting in the oxidation of the dye. Injected electrons in the conduction band of $TiO_2$ are transported between $TiO_2$ nanoparticles with diffusion toward FTO.

$$S^* \rightarrow S^+ + e^-(TiO_2)$$

The oxidized dye ($S^+$) accepts electrons from $I^-$ ion mediator (redox electrolyte), regenerating the ground state (S). $I^-$ is oxidized to the oxidized state, $I_3^-$.

$$2S^+ + 3I^- \rightarrow 2S + I_3^-$$

The oxidized redox mediator, $I_3^-$, diffuses toward the counter electrode and is reduced to $I^-$ ions.

$$I_3^- + 2e^- \rightarrow 3I^-$$

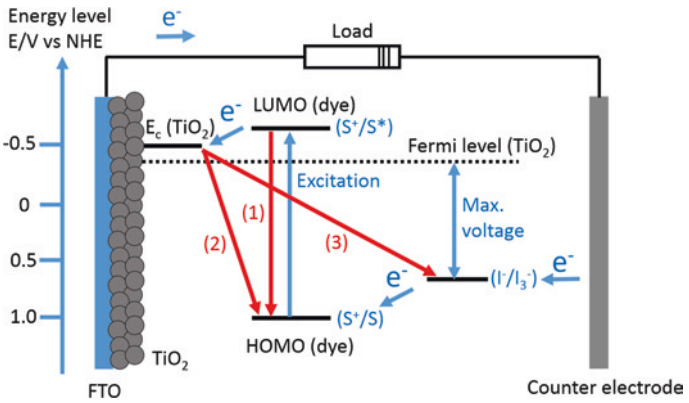


**Fig. 9.11** Energy-band diagram and operation principle of a typical DSSC. The electron transfer processes are illustrated with blue arrows. Unfavorable back-reaction processes are illustrated with red arrows

Thus, the electric power is generated. The obtained photocurrent is determined by the energy gap of the dye. The open-circuit voltage produced is determined by the energy gap between the Fermi level of $TiO_2$ and the potential of electrolyte. In theory, the smaller LUMO-HOMO energy gap of dye is, the larger photocurrent will be achieved. However, the LUMO and the HOMO energy levels of the dye need to be appropriately designed with the consideration of the energy levels of $TiO_2$ and electrolyte. For the efficient charge injection, it requires a driving force of about 100–200 meV [10]. In order to inject electrons effectively, the LUMO level of dye must be sufficiently negative in comparison with the conduction band of $TiO_2$. Also, in order to accept electrons effectively, the HOMO level of dye must be sufficiently positive in comparison with the potential of electrolyte.

Unfavorable back-reaction processes in a typical DSSC include (1) the relaxation of the excited state of dye, (2) the charge recombination between the injected electrons and the dye cations, and (3) the charge recombination between the injected electrons and the electrolyte [11], as shown with red arrows in Fig. 9.11. Electron injection from the dye into the $TiO_2$ photoelectrode typically happens in the femtosecond to picosecond time scale [12]. The process is much faster than the charge recombination process, which typically happens in the micro to millisecond time scale. In addition, the back reaction of a conduction band electron to the oxidized dye is much slower than the reduction of the oxidized dye by the electrolyte. Thus this cell structure gives the electrons sufficient time to be collected by the contacts.

### *9.2.5 Tandem Solar Cells*

The above solar cells all use single junction. The single-junction solar cells all have their output voltage limited by the bandgap of materials because of

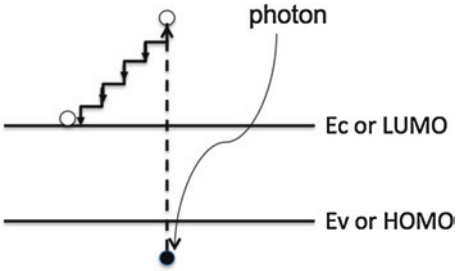


**Fig. 9.12** Illustration of electron-phonon scattering process that causes electron to lose energy and relax to the band edge or the LUMO level

significant thermal loss. As illustrated in Fig. 9.12, as the photon energy is much larger than the bandgap, the electron will transit to an energy level much higher than the conduction-band edge of the semiconductors or the LUMO level of organic material. This high-energy electron will then experience very fast electron-phonon scattering. The energy of electron will be transferred to phonons until its energy reaches the band edge or it becomes bounded in the exciton. The holes will experience similar process, too. Such process is very fast, only a few picoseconds. Therefore, before electrons and holes transport to the external circuit, they have already relaxed to the band edges or form excitons. As a result, lots of energy will be lost. For example, if the photon energy is 2.24 eV, being absorbed by Si, the thermal loss will be 1.12 eV because Si has a bandgap of 1.12 eV. The thermal loss will be as large as 50 %.

To reduce the thermal loss, one can use large bandgap materials. However, those materials can then only absorb light with energy larger than the bandgap. Sunlight covers a wide range of optical spectrum. As shown in Fig. 9.13 [13], the solar spectrum covers from 300 nm up to 4000 nm. If the entire solar spectrum is converted to current, there will be a large current density of around 62 mA/cm$^2$. Nonetheless, large bandgap materials can absorb only a small portion of light. As a result, there is a conflicting reality. Large bandgap will lead to small photo current, while small bandgap will lead to small output voltage due to the thermal loss. Consequently, the output voltage and the output current are contradictory. A tradeoff has to be made. The evaluated maximum device efficiency is about 31 % from a single junction solar cell.

To surpass this limitation due to the tradeoff, multiple junctions are proposed. Each junction is only responsible for absorbing a short range of solar spectrum. To absorb a broad spectrum of the sunlight, each junction is certainly made of one type of semiconductor that has different bandgap from other semiconductors used for other junctions. The layout is schematic shown in Fig. 9.14. Solar cell I is made of the material that has the largest bandgap. Solar cell II is made of the material that has the second largest bandgap. Others follow the same order.

Each junction of solar cell in the multi-junction structure is similar to the single junction described previously. When they are made of tandem cells, the neighboring cells have their p-side and n-side connected together. As a result, the holes from the p-side will recombine with the electrons in the n-side of another solar

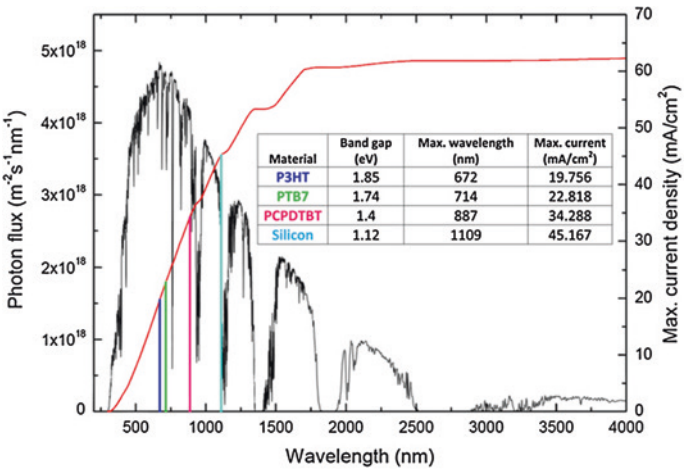


**Fig. 9.13** solar spectrum [13]

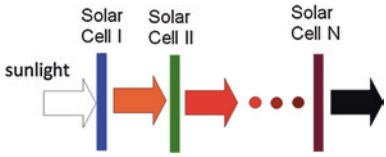


**Fig. 9.14** Layout of multi-junction solar cells

cell. It has to be one to one correspondence. That is, each hole will recombine with one electron. If there are more holes or electrons, they will transport to the neighboring cell and eliminate the holes or electrons generated there, leading to the reduction of the photo current. This will result in the waste of photo-generated carriers in certain cells and so the power conversion efficiency. To maximize the power conversion efficiency, each cell should have the same current. Therefore, the tandem cells need very delicate design. Each cell should absorb the same photon number of sunlight and generate the same amount of electron-hole pair.

## 9.3 Progress of Various Types of Solar Cells

In this section, we will introduce various types of solar cells and their recent progress.

### *9.3.1 Crystalline Si Solar Cells*

Crystalline Si solar cells are the most conventional type and are the main stream of solar-cell industry. The fabrication starts from the formation of raw Si materials,

which are then further refined to a high purity. The high-quality Si are made as ingots, which are sliced to Si wafers using diamond saws. Afterwards, standard semiconductor processing steps are applied to form p-n junction, metal contacts, and then cells. The p-n junction will have a built-in electrical field, so as electrons and holes are generated, they are pulled away and move to opposite electrodes, following the principles described previously. Currently the best efficiency of single-crystalline Si solar cells and the multiple-crystalline solar cells is 25 and 20.4 %, respectively [14]. The overall cost of using solar cell to harvest solar energy and to convert to electricity is still larger than using fossil energies, so quite many efforts are still required to make solar energy using crystalline Si solar cells become a significant portion of future energy supplies.

### *9.3.2 Amorphous Si Solar Cells*

Amorphous Si (a-Si) solar cells are usually with the p-i-n structure. The p-layer and the n-layer provide the function of creating a built-in electrical field. The i-layer is sandwiched between the p-layer and the n-layer. It is responsible for light absorption. The thickness of this layer is around 0.2–0.5 um. Because the a-Si has a larger bandgap than crystalline, it absorbs photons with energy larger than 1.5–1.8 eV, depending on the fine structure of a-Si. This energy is larger than 1.1 eV, bandgap of Si, so the absorption spectrum of a-Si is narrower than crystalline Si, but it has a much larger absorption coefficient, $10^4$–$10^5$ $cm^{-1}$. Increasing the thickness of the i-layer can enhance the light absorption, but will also increase the probability of electron-hole recombination and hence decrease the photo-current and the open-circuit voltage.

The p-, n-, and i-layers are usually deposited using plasma-enhanced chemical vapor deposition (PECVD). They can be placed on stainless-steel foils, glass substrates, or plastics. If the flexible substrates like stainless-steel foils or plastics are used, the fabrication can be done with roll-to-roll production, which will have great advantages in mass-production, shipping, and implementation on the house roofs and racks in the fields. The a-Si solar cells still use transparent conducting oxide for light transmission and current conduction. Also they highly rely on huge vacuum processing. Thus the overall cost is only slightly lower than crystalline solar cells. In addition, the best efficiency of a-Si solar cells is only slightly larger than 10 % [14], making it less preferable than crystalline Si solar cell for practical implementation.

### *9.3.3 III-V Semiconductor Solar Cells*

The III-V semiconductor solar cells are made of compound semiconductors that consist of group III and group V chemical elements in the periodic table. Typical

III-V compound semiconductors used for solar cells are based on GaAs, InP, and GaN. Because they are also semiconductors, the operation principle is similar to crystalline Si solar cells, as described previously. A great advantage of III-V compound semiconductors is that the bandgap can be engineered using different ratio of III-V chemical elements. For example, AlGaAs has the bangap between AlAs and GaAs, depending on the chemical ratio between Al and Ga. Also, most of the III-V compound semiconductors are direct-bandgap materials, so their light absorption coefficient is much larger than that of Si. It can be as large as $10^5$ $cm^{-1}$, so 95 % of light can be absorbed with only 1 um of thickness. The disadvantage of the III-V semiconductor solar cells is that those semiconductors are usually grown using metalorganic vapour phase epitaxy (MOCVD) or molecular beam epitaxy (MBE), which is very expensive. Therefore, the cost of III-V semiconductor materials is very high. To reduce the material cost, III-V semiconductor solar cells are usually used in concentrated solar system, which a lens of concentrator is applied to collect a large area of sunlight to be focused on the chip of the III-V semiconductor solar cells.

On the other hand, the epitaxial growth and the possibility of bandgap engineering make the III-V semiconductor solar cells most likely formed in tandem structures, so extremely high efficiency is possible. So far, the highest efficiency is achieved from the III-V tandem solar cells in a concentrated solar system [14].

### *9.3.4 CIGS Thin-Film Solar Cells*

CIGS thin-film solar cells are made of compound semiconductors that consist of four different chemical elements: copper, indium, gallium and selenium. The n-type or p-type of CIGS compound is controlled from the ratio of $Cu_2Se$ and $In_2Se_3$. It is also a direct-bandgap semiconductor, so has a large absorption coefficient, ~$10^5$ $cm^{-1}$ and about 1-um of thin film could absorb about 95 % of sun light. CIGS can be deposited on flexible substrates, so roll-to-roll production is possible, making it very attractive for relatively easy mass-production, shipping, and implementation on the house roofs and racks in the fields. In addition, a very good efficiency of 19.6 % [14] has been demonstrated, so it attracts significant attention recently. However, it also faces some challenges. It uses toxic chemical of Cd and Se. In addition, the storage of In on earth is small, limiting the possible expansion of CIGS solar cells to a very large scale. The processing steps and controls to obtain good CIGS crystal for high efficiency solar cells are complicated and involve expensive vacuum apparatuses.

### *9.3.5 CdTe Thin-Film Solar Cells*

CdTe thin-film solar cells are formed from p-type CdTe compound semiconductor and the n-type CdS compound semiconductor. The p-type CdTe is about

2 um, while the n-type CdS is only 0.1 um. Therefore, light is mainly absorbed by the CdTe layer, which has absorption coefficient slightly less than $10^5$ $cm^{-1}$. Its bandgap is about 1.45 eV, so it is able to absorb light from UV to about 855 nm. Because either the p-type CdTe layer or the n-type CdS layer consists of only two chemical elements, the material processing is simpler than CIGS. Its best efficiency is also 19.6 % [14]. Now some portion of commercial solar panels is made of CdTe thin-film solar cells. However, there are still some concerns. First, it uses Cd, which is toxic, so recycling Cd material is important to avoid environmental contamination. Second, the storage of Te element on earth is small, so imposing its limitation on possible expansion to a very large scale.

### *9.3.6 Dye-Sensitized Solar Cells*

In dye-sensitized solar cells (DSSCs), dye molecules are used for light absorption. However, dye is not a conductive material, so the layer of dye has to be very thin, so photo-generated electrons and holes can be transferred to their neighboring conducting layers. Because the layer of dye is very thin, it absorbs very small amount of light. To increase the light absorption, porous structure of electron-conducting materials, e.g., $TiO_2$, is used and dye molecules are adsorbed on its surface. As the overall thickness of the porous electron-conducting material is thick enough, significant absorption of light can be achieved. Fortunately, quite mature technologies had already developed to fabricate the porous electron-conducting material ($TiO_2$) and to adsorb dye molecules. Also, to achieve good contact of dye with the hole transportation material, liquid electrolyte containing $I^-$ and $I_3^-$ ions is used. Such DSSCs exhibit efficiency of 11.9 % [15]. The fabrication steps are simple. Roll-to-roll production is also possible. Thus it has been deemed as a very promising technique. However, the use of liquid electrolyte makes it inconvenient to use. As a result, solid-state electrolytes become an attractive direction of improvement. Solid-state DSSCs now could have the best efficiency of 10.2 %. As long as the efficiency is further increased from the solid-state DSSCs, it should be pretty promising for practical applications. Nonetheless, its efficiency does not have significant progress over these years.

Some research groups replace the dye molecules with the perovskite materials in the similar structure. Because the perovskite material has better conductivity than dye molecules, no porous structure is required. Hence, its fabrication is even simpler than conventional DSSCs. Perovskite solar cells can be fabricated using solution process or evaporation. The solution-processed ones can have the efficiency of 11.4 % and 19.3 % [16, 17], while the evaporated ones have the efficiency of 15.4 % [18]. The only concern is the use of heavy metal Pb in perovskite, giving some risk of environmental contamination and increased cost of recycling.

### *9.3.7 Organic Solar Cells*

Organic solar cells have the advantages of low cost, light weight, simple process, and flexibility. Compared to semiconductor types, organic solar cells can be fabricated with solution processes such as spin-coating, spray, screen-printing, dip-coating, blade coating, and so on. They can certainly be fabricated using roll-to-roll production. However, due to the short diffusion length of excitons in organic polymers, some nano-morphology of inter-link configuration is necessary. It is not easy to control. Currently the best efficiency of organic solar cells is around 10 % [14], but is limited to small areas. Large-area organic solar cells do not have high efficiency although they have great potential of low lost. Also, the easy interaction of organic material with air and moisture makes organic solar cells short lifetime, so encapsulation will be necessary.

## References

1. M. Riordan, L. Hoddeson, The origins of the pn junction. IEEE Spectr. **34**, 46–51 (1997)
2. D. Chapin, C. Fuller, G. Pearson, A new silicon p-n junction photocell for converting solar radiation into electrical power. J. Appl. Phys. **25**, 676–677 (1954)
3. G.A. Chamberlain, Organic solar cells: a review. Solar Cells **8**, 47–83 (1983)
4. C.W. Tang, Two-layer organic photovoltaic cell. Appl. Phys. Lett. **48**, 183–185 (1986)
5. J.H. Schön, Ch. Kloc, B. Batlogg, Efficient photovoltaic energy conversion in pentacene-based heterojunctions. Appl. Phys. Lett. **77**, 2473–2475 (2000)
6. F. Gao, Y. Wang, D. Shi, J. Zhang, M. Wang, X. Jing, R. Humphry-Baker, P. Wang, S.M. Zakeeruddin, M. Grätzel, Enhance the optical absorptivity of nanocrystalline $TiO_2$ film with high molar extinction coefficient ruthenium sensitizers for high performance dye-sensitized solar cells. J. Am. Chem. Soc. **130**, 10720–10728 (2008)
7. S. Ito, S.M. Zakeeruddin, R. Humphry-Baker, P. Liska, R. Charvet, P. Comte, M.K. Nazeeruddin, P. Péchy, M. Takata, H. Miura, S. Uchida, M. Grätzel, High-efficiency organic-dye-sensitized solar cells controlled by nanocrystalline-$TiO_2$ electrode thickness. Adv. Mater. **18**, 1202–1205 (2006)
8. C. Pérez León, L. Kador, B. Peng, M. Thelakkat, Characterization of the adsorption of Ru-bpy dyes on mesoporous $TiO_2$ films with UV-Vis, Raman, and FTIR spectroscopies. J. Phys. Chem. B **110**, 8723–8730 (2006)
9. J.F. Endicott, H.B. Schlegel, M.J. Uddin, D.S. Seniveratne, MLCT excited states and charge delocalization in some ruthenium-ammine-polypyridyl complexes. Coord. Chem. Rev. **229**, 95–106 (2002)
10. http://www.diss.fu-berlin.de/diss/servlets/MCRFileNodeServlet/FUDISS_derivate'_000000002568/02_2.pdf?hosts=
11. M.V. Martínez-Díaz, M. Ince, T. Torres, Phthalocyanines: colorful macroheterocyclic sensitizers for dye-sensitized solar cells. Monatshefte für Chemie-Chemical Monthly **142**, 699–707 (2011)
12. D. Kuciauskas, J.E. Monat, R. Villahermosa, H.B. Gray, N.S. Lewis, J.K. McCusker, Transient absorption spectroscopy of ruthenium and osmium polypyridyl complexes adsorbed onto nanocrystalline $TiO_2$ photoelectrodes. J. Phys. Chem. B **106**, 9347–9358 (2002)
13. M. Wright, A. Uddin, Organic-inorganic hybrid solar cells: a comparative review. Solar Energy Mater. Solar Cells **107**, 87–111 (2012)

14. M.A. Green, K. Emery, Y. Hishikawa, W. Warta, E.D. Dunlop, Solar cell efficiency tables (version 42). Progress in Photovoltaics **21**, 827–837 (2013)
15. I. Chung, B. Lee, J. He, R.P.H. Chang, Mercouri G. Kanatzidis, All-solid-state dye-sensitized solar cells with high efficiency. Nature **485**, 486–490 (2012)
16. G.E. Eperon, V.M. Burlakov, P. Docampo, A. Goriely, H.J. Snaith, Morphological control for high performance, solution-processed planar heterojunction perovskite solar cells. Adv. Funct. Mater. **24**, 151–157 (2014)
17. H. Zhou, Q. Chen, G. Li, S. Luo, T.-B. Song, H.-S. Duan, Z. Hong, J. You, Y. Liu, Y. Yang, Interface engineering of highly efficient perovskite solar cells. Science **345**, 542–546 (2014)
18. M. Liu, M.B. Johnston, H.J. Snaith, Efficient planar heterojunction perovskite solar cells by vapour deposition. Nature **501**, 395–398 (2013)